

**Radar Characteristics of Wintertime Storms in the
Colorado Rockies**

by
R. William Furman

Technical Paper No. 112
Department of Atmospheric Science
Colorado State University
Fort Collins, Colorado

**Colorado
State**
University

**Department of
Atmospheric Science**

Paper No. 112

RADAR CHARACTERISTICS OF WINTERTIME
STORMS IN THE COLORADO ROCKIES

by
R. William Furman

This report was prepared with support from
the National Science Foundation
Grant No. GP-4750
Principal Investigator, Lewis O. Grant

Department of Atmospheric Science
Colorado State University
Fort Collins, Colorado

July 1967

Atmospheric Science Paper No. 112

ABSTRACT

The objective of this paper is to present the results of an investigation of the physical features of orographic clouds. Cloud systems accompanying three winter storms were observed as they passed over the Colorado Rockies, utilizing both horizontal and vertical scanning 3 cm radar. A cloud model based on published information on orographic clouds was constructed and tested.

The most intense precipitation and dense clouds were found in the vicinity of the tops of mountains and ridges. Mean cloud depth was found to range between 4,000 and 9,000 ft. Cloud bases were in all cases within 500 to 1,000 ft of the 12,000 ft msl mountain laboratory. The mean cloud tops occurred from 16,000 to 21,000 ft with occasional tops reaching to 27,000 ft msl.

The movement of echoes was found to agree with the 500 mb wind velocity. From this it was concluded that the 500 mb wind is the steering wind for convecting elements known to exist in these cloud masses.

Harmonic analysis of the solid cloud tops and maximum horizontal echo ranges has revealed a periodic passage of convective elements over Chalk Mountain. These elements are thought to be organized into lines. The spacing of the elements was observed to be 110 miles between centers. Corresponding to the

passage of convective elements over the station, the precipitation intensity has been observed to vary by an order or magnitude.

R. William Furman
Atmospheric Science Department
Colorado State University
July, 1967

ACKNOWLEDGEMENTS

The author wishes to express gratitude to Professor Lewis O. Grant for his helpful suggestions while this research was being conducted. An expression of appreciation is also due Donald Cobb for the many hours spent calibrating the radar equipment. Thanks also go to my wife, Susan, for her help, encouragement, and tolerance during this investigation.

This research was sponsored by the National Science Foundation under Contract GP 4750.

This material is based upon a thesis submitted as partial fulfillment of the requirements for the Master of Science Degree at Colorado State University.

TABLE OF CONTENTS

	Page
TITLE PAGE	i
ABSTRACT	ii
ACKNOWLEDGEMENTS	iv
LIST OF TABLES	vii
LIST OF FIGURES	viii
INTRODUCTION	1
Objective	3
Model	4
PROCEDURE	5
DESCRIPTION OF AREA AND CLIMATOLOGY	6
INSTRUMENTATION	10
Search Radar	10
Vertical-Pointing Radar	11
DATA REDUCTION TECHNIQUES	13
Horizontal Echo Patterns	13
Vertical Echo Patterns	14
Rate of Echo Movement	17
Precipitation Intensities	19
Error Analysis	21
ANALYSIS	25
Horizontal Echo Distribution	25
Vertical Profile	26
Movement.	27
Convective Activity	28

LIST OF TABLES

TABLE		PAGE
1	Climatological data for Climax, Colorado based on records from 1951-1961	8
2	Modified SO-12 radar characteristics	10
3	Percentage distribution of the total echo area for each gain step, $P_j(k)$	14
4	Measured echo velocities and 500 mb wind velocity	19

LIST OF FIGURES

FIGURE		PAGE
1	Location of Climax, Colorado	7
2	Distribution of $P_j(k)^*$ with range for each gain step.	15
3	Simultaneous variation of precipitation intensity, solid cloud tops and maximum horizontal range	16
4	Schematic of A-scope showing the relative positions of absolute tops and solid tops . . .	18
5	500 mb chart sequence showing radar echo movement	20
6	Amplitude contributions of harmonic wave components to the total wave form.	31
7	Receiver linearity curve	47
8	SO-12 radar calibration curve using a 12-inch corner reflector	50
9	Calibration curve for modified SO-12 3cm radar	51

INTRODUCTION

Under the auspices of the National Science Foundation, Colorado State University is investigating the feasibility of increasing winter precipitation through weather modification in the Central Colorado Rockies. The outcome of this investigation will be the evaluation of the results of a randomized cloud seeding program and a study of the physical processes related to the precipitation mechanism in orographic clouds.

The detailed mesostructure of the cloud patterns over the Rocky Mountain orographic barrier is not known. Ludlam (1955) describes clouds moving over mountains as those formed by the air forced upward and often superimposed upon an already-existing system of shallow cumulus or stratocumulus clouds. Over the mountains these clouds become a continuous layer with a considerable increase in thickness. Inside these clouds there exist continuous irregular or convective stirring motions. Ludlam also describes the density of the droplet cloud and the mean ice particle size as increasing toward the summit of the mountain and decreasing again to the lee of the summit.

Elliott and Hovind (1964) describe the presence of convective motions in the form of banded structures embedded in the orographic rain clouds of the Santa Barbara area of Southern California. The

bands were described as being 20 to 40 miles wide and centered some 30 to 60 miles apart.

A limited amount of information has been accumulated on the structure of snowstorm cloud patterns and virtually none on the cloud structure in an orographic snowstorm. Gunn et al. (1954), Wexler (1955) and Langleben (1956) have discussed the structure of frontal snowstorms. They describe in detail the existence of generating elements from which snow appears to fall. Grant et al. (1965) report convective activity in the cloud patterns observed over the Central Colorado Rockies, but at the time of the investigation were unable to determine whether or not this activity was organized into bands. Gunn et al. (1954) and Douglas et al. (1957) have reported the mean thickness of snowstorms near Montreal, Canada, to be 10,000 ft with the tops of the storm near 13,000 ft mean sea level (msl). Virtually no information on the thickness of orographic clouds is available.

OBJECTIVE

The objective of this investigation is to describe several features of the orographic clouds which occur in winter storms over the Colorado Rockies. These features will then be compared to a conceptual model of a winter orographic cloud assembled from published information. The emphasis will fall on four primary areas of investigation:

1. The horizontal distribution of cloud and precipitation patterns.
2. Features of the cloud vertical profile such as the thickness and the mean height of the cloud tops.
3. The cellular structure of the orographic cloud and the relation of the cells to precipitation intensity.
4. The movement of the clouds as compared to the winds aloft.

MODEL

As an aid in this investigation, it is convenient to construct a conceptual model of an orographic storm.

The forced lifting of air over an orographic barrier results in a continuous layer of clouds with thicknesses ranging up to 10,000 ft. In the orographic updraft under natural (non-seeded) conditions, saturation with respect to liquid water is maintained at the temperature of the cloud allowing snow crystals to grow at a maximum rate. In light to moderate winds the growth rate of ice crystals is usually sufficient for substantial portions of the particles to be precipitated upwind of, or on, mountain peaks. At stronger velocities, 40 mph or greater, it is possible for the precipitation to be carried beyond the mountain top and at least partially evaporated in the descending air to the lee of the mountain. Under this condition, the particles do not have sufficient time to grow to a size large enough to fall from the cloud (Ludlam, 1955).

Inside the cloud, stirring or convective motions exist in organized fashion. These centers of convective activity or cells are organized into bands (Elliott and Hovind, 1964) which move within the orographic cloud mass along the 500 mb wind vector. The continuous flux of water vapor into the cells by the mixing and stirring motions results in a precipitation rate higher than the mean precipitation rate of the orographic cloud mass.

PROCEDURE

Three major storms that crossed the Rocky Mountains in the winter of 1966 were surveyed with an X-band (3 cm) search radar and an X-band vertical-pointing radar. Both radars are installed in a laboratory on top of Chalk Mountain in the center of the Colorado Rockies. These storms occurred on March 21, April 18 and 19, and April 22, 1966, and each storm provided at least six hours of echoes on the radars. To supplement the radar information, measurements of the rate of precipitation were taken at the High Altitude Observatory (HAO) located near the base of Chalk Mountain. These measurements were made by periodically weighing the amount of snow deposited on a plastic sheet of known area. The features of the clouds were investigated by observing the time-lapse films of the radar indicators and the change of precipitation intensity.

DESCRIPTION OF AREA AND CLIMATOLOGY

This field study was conducted in a section of Central Colorado near Climax where the Continental Divide is oriented east-west for a short distance. The primary orographic features consist of several mountain ranges oriented north-south. Approximately 4 miles to the east of Chalk Mountain is the Tenmile Range which has an average maximum elevation of 12,500 to 13,000 ft msl with several peaks reaching to over 14,000 ft. Six miles to the east of Tenmile Range, the Continental Divide turns toward the north along Hoosier Ridge. Three miles to the west of Chalk Mountain, Chicago Ridge extends to 12,500 ft but has a north-south dimension of only 8 miles. Twelve miles beyond Chicago Ridge, the Sawatch Range, with peaks reaching over 14,000 ft, extends south along the Continental Divide. Chalk Mountain is part of a small range of mountains, the Gore Range, located between Chicago Ridge and Tenmile Range, and has a mean maximum elevation of nearly 12,000 ft. Figure 1 is a map of the area showing these major topographic features. HAO is located on the northeast side of Chalk Mountain at an elevation of 11,400 ft.

With such topography it may be seen that a southwesterly flow of air must pass over a section of the Continental Divide before reaching Chalk Mountain. It is believed that under these conditions a substantial amount of moisture is deposited on the windward side of



Figure 1. Location of Climax, Colorado

the Continental Divide before it reaches Chalk Mountain. Air moving in from the northwest, however, is unobstructed until it reaches the Divide at and to the northeast of Chalk Mountain.

Table 1 lists climatological data for Climax from U. S. Weather Bureau Climatological Data for the period 1951-1961. Grant et al. (1965) reported that approximately 70% of the total precipitation falls at intensities of 0.03 in/hr or less. They also found that the precipitation intensity is only 0.01 in/hr or less for 45% of the time.

TABLE 1

Climatological data for Climax, Colorado
based on records from 1951-1961

	Winter Nov. -Apr.	Summer May-Oct.	Annual
Mean Precipitation (in)	14.14	9.94	24.08
Mean Temperature (°F)	18.6	43.8	31.2
Mean No. of Days with Precipitation 0.10"	46	33	79

The winter synoptic weather pattern is dominated by a long-wave ridge positioned over the Western U.S. which produces fair weather over the Rockies. This mean pattern is often disturbed by large traveling cyclones, which move over the mountains leaving behind important amounts of precipitation in the form of snow.

From Table 1 it can be seen that the majority of the annual precipi-

tation associated with the cyclones occurs at Climax in the winter. During the summer months, afternoon convective showers occur almost daily and account for most of the summer precipitation.

INSTRUMENTATION

The equipment at the laboratory on Chalk Mountain includes two modified SO-12 M/N X-band radars. These radar systems are primarily used to observe precipitation patterns from which the mesoscale structure and associated cloud patterns of storms crossing the Rocky Mountains may be deduced.

Search Radar

An SO-12 M/N radar modified for a circular antenna and a Plan Presentation Indicator (PPI) is the instrument used for surveillance of the precipitation patterns. The PPI displays ranges of 40K, 80K and 120K yards. The characteristics of the radar system are given in Table 2. This radar is equipped with a stepped gain which

TABLE 2
Modified SO-12 radar characteristics

Power transmitted (P_t)	50 K watts
Wave length (λ)	3 cm
Pulse length (h)	1.0 μ sec
Pulse repetition frequency (PRF)	465 sec
Antenna shape	circular
Antenna diameter	6 feet
Vertical beam width (1/2 power points)(ϕ)	1°
Horizontal beam width (1/2 power points)(θ)	1°
Minimum detectable signal (MDS)	3.16×10^{-13} watts

can be operated either manually by the operator or automatically.

This mechanism decreases the sensitivity of the receiver by selected increments of power. In the automatic mode the gain is reduced with each rotation of the antenna and is automatically reset to full gain on any preset step up to six steps. Each gain step may be adjusted to attenuate the incoming signal by any desired amount. For the three storms considered, the signal was reduced by each gain step as follows:

<u>Gain Step</u>	<u>Power loss to signal (dbm)</u>
1	0.0
2	1.0
3	2.3
4	4.0
5	6.0

By providing a means of locating areas of different precipitation intensities, the stepped gain mechanism is a method of investigating many problems relating to cloud and precipitation intensities.

The search radar was calibrated as outlined by Atlas and Mossop (1960) (see Appendix).

Vertical-Pointing Radar

An SO-12 radar is also being used as a vertical-pointing radar to obtain information concerning the vertical structure of cloud patterns passing over the station. This radar was also modified for

a circular antenna but has an A-scope indicator. The range is displayed on the horizontal axis as a series of time markers which denote intervals of height equal to one mile. These markers are used to estimate the height of points of interest to the nearest 1,000 ft. The intensity of the echo is measured along the ordinate.

Presentation from both systems have been mounted in a manner to allow them to be photographed simultaneously with a 16 mm Keystone time-lapse camera. The shutter is normally open, and the film is advanced with each rotation of the search antenna which is approximately 2 rpm. The time and date are also displayed in the same field of view.

DATA REDUCTION TECHNIQUES

Horizontal Echo Patterns

Horizontal characteristics of the precipitation patterns may be investigated using plan position patterns. The plan position data used in this investigation was obtained from the film by taking a series of tracings at half-hour intervals. The tracings were obtained by projecting the film with a stop-motion projector on sheets of paper and tracing all the echoes. One such tracing was drawn for each gain step until a cycle was completed and the step returned to full gain.

The amount of echo area occurring in each of the areas between consecutive specified ranges was estimated as a percentage of the total echo area on each tracing. This percentage shall be designated as $P_j(k)$ where \underline{j} denotes the area between range circles and \underline{k} is the gain step. For a given \underline{k} , $P_j(k) = 100$. The areas considered are those between the radii 1-2, 2-3, 3-4, 4-5, 5-7, 7-10 nautical miles (n mi) which corresponds to $j = 1, 2, 3, 4, 5$ and 6 respectively. Since 99% of the useable echo area occurred within 1 to 10 n mi, no echoes outside this area were considered. Table 3 shows the distribution of $P_j(k)$ for all \underline{j} and \underline{k} . To remove the effect of the difference in the \underline{j} areas it is convenient to consider $P_j(k)$ per unit area \underline{j} , $(P_j(k)/A_j)$, which will be denoted as $P_j(k)^*$.

TABLE 3
Percentage distribution of the total echo area
for each gain step, $P_j(k)$

k	j =	1	2	3	4	5	6
1		47	27	15	5	4	2
2		49	27	14	4	4	2
4		56	28	11	3	2	
5		69	25	6			
6		67	22	11			

The distribution of $P_j(k)^*$, averaged for the three storms is shown as a function of range in Figure 2. Averages were used under the assumption that the averaging process would illuminate the characteristics typical to all three storms and smooth out the individual characteristics. This is desirable since we wish, in this particular investigation, to study those facets common to a large number of disturbances crossing Central Colorado.

The observed maximum echo range was plotted at fifteen-minute intervals for comparison with the variation of the vertical echoes (Figure 3).

Vertical Echo Patterns

The mean height of the cloud tops observed over the Colorado Rockies has been estimated from the height of the absolute radar tops of the three storms. The absolute tops of the clouds were

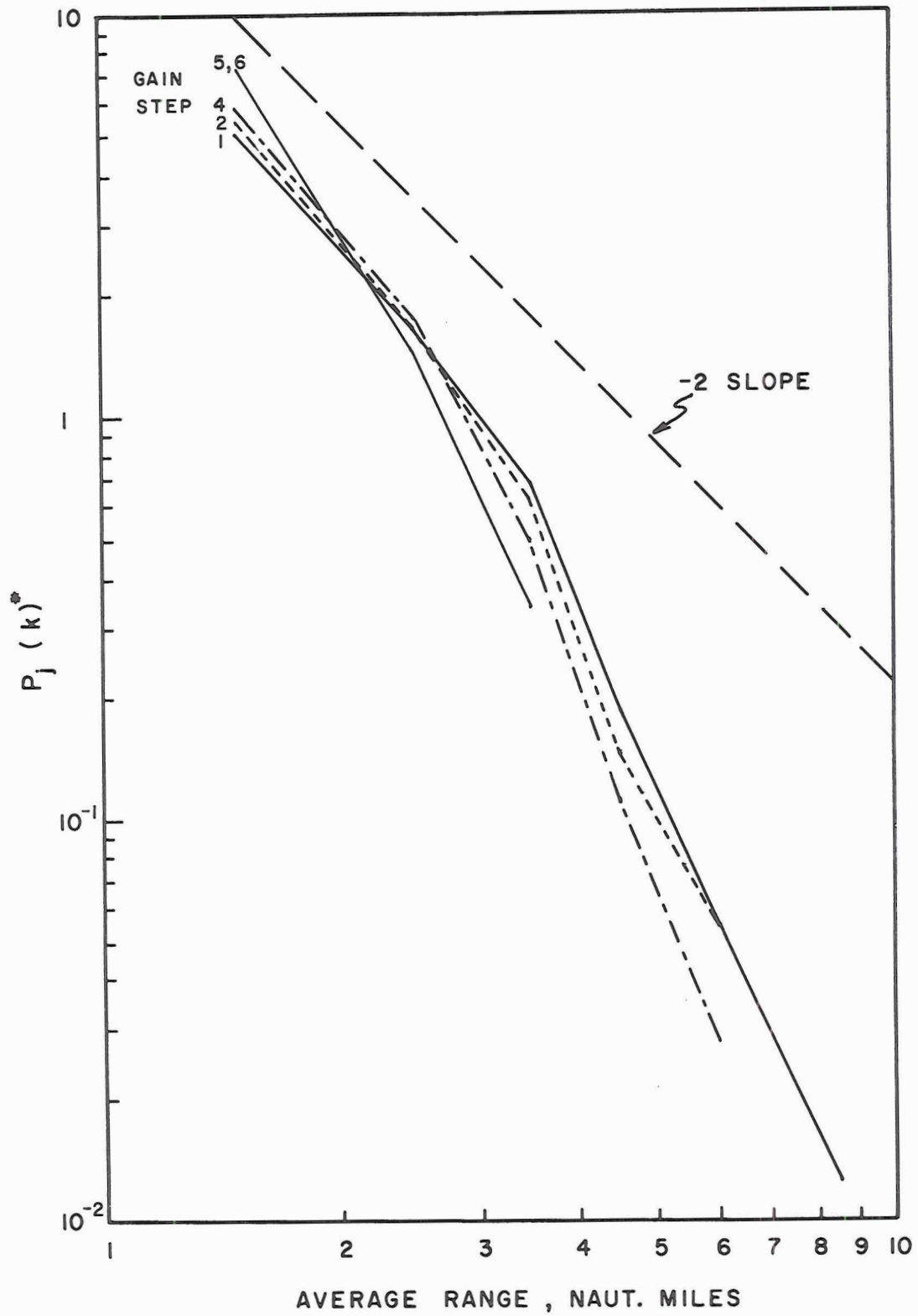


FIGURE 2 DISTRIBUTION OF $P_j(k)^*$ WITH RANGE
FOR EACH GAIN STEP

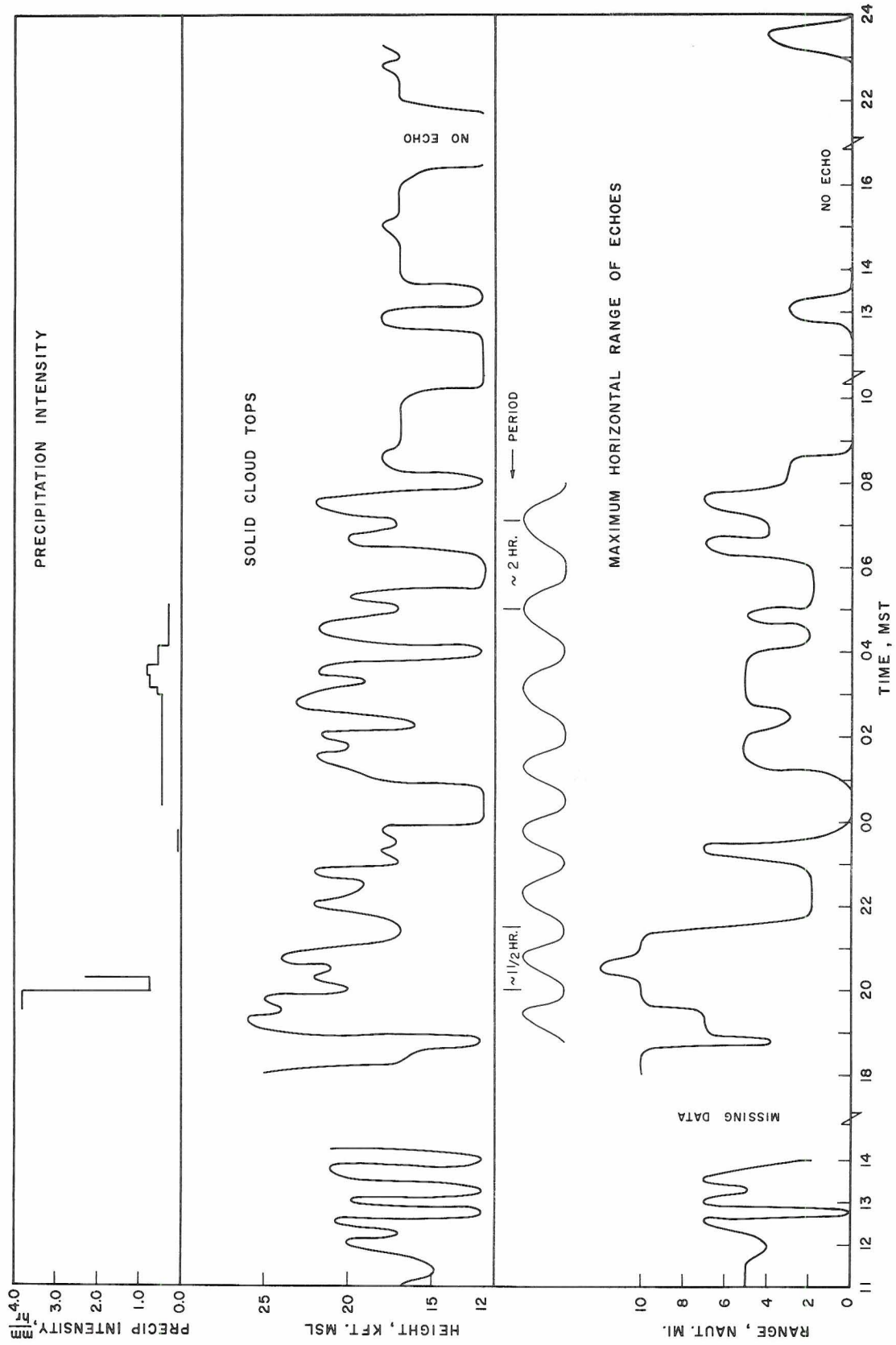


FIGURE 3 SIMULTANEOUS VARIATIONS OF PRECIPITATION INTENSITY, SOLID CLOUD TOPS AND MAXIMUM HORIZONTAL RANGE OF ECHOES

determined by the height of the minimum detectable signal on the A-scope. These measurements were determined at half-hour intervals and the mean heights of the absolute tops for the three storms were found to vary from 16,000 ft to 21,000 ft msl. Extremes were observed to 27,000 ft msl.

At fifteen-minute intervals the height of the solid radar tops were determined for the storm of April 18 and 19. This storm was chosen for investigation because of its long and essentially continuous radar record. The solid radar cloud top has been defined as the maximum height at which the intensity of the vertical signal decreased below an arbitrarily designated level. This arbitrary level was set high enough to eliminate the very low intensity signals and noise which may affect the estimation of the absolute tops and remained constant throughout the investigation. The time variation of the solid tops is shown in Figure 3. Figure 4 shows the relative locations of the absolute and solid tops on an A-scope.

Rate of Echo Movement

To investigate the movement of the echo patterns and determine the relative contributions of drift and propagation, tracings 5 to 7 minutes apart were made of selected echoes. The echo velocity was determined by measuring the distance and direction of movement of the echo center. Care was taken to select echoes

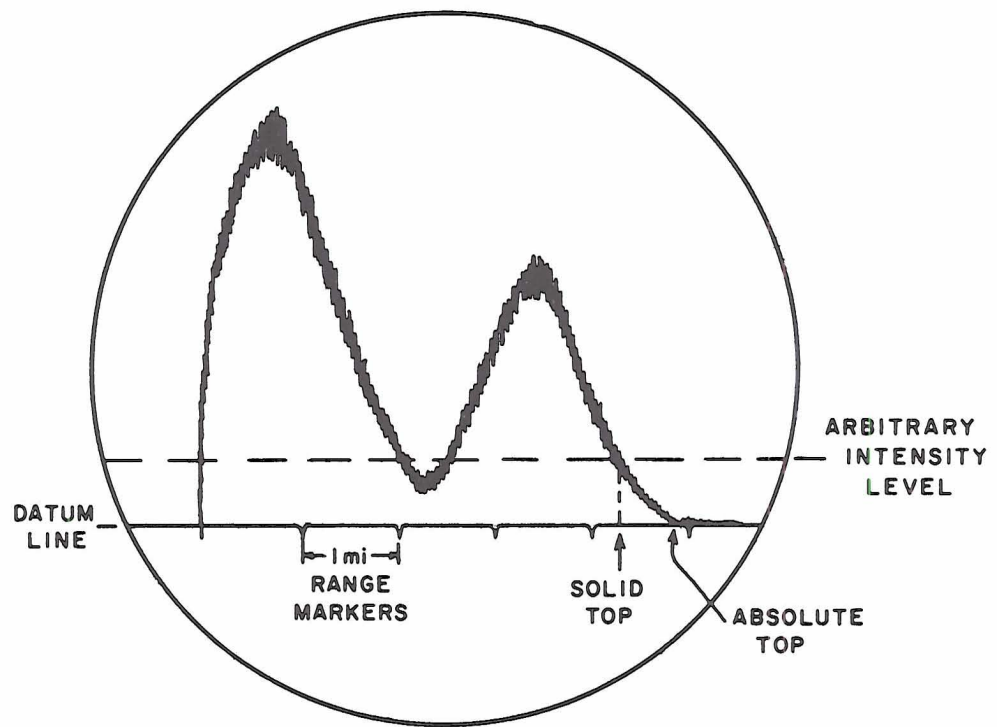


FIGURE 4 SCHEMATIC OF A-SCOPE SHOWING RELATIVE POSITIONS OF ABSOLUTE TOP AND SOLID TOP

which had sufficient portions of their boundaries visible to allow the center of the echoes to be determined.

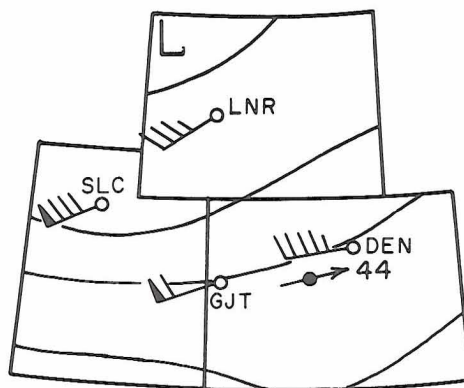
The echo velocities and Climax 500 mb wind velocity for three given times during the storm of March 22 and one time for April 19 are shown in Table 4. The echo velocities for March 22 are also shown in Figure 5 plotted on the appropriate 500 mb charts for comparison with the 500 mb wind velocity.

TABLE 4
Measured echo velocities and 500 mb wind velocity

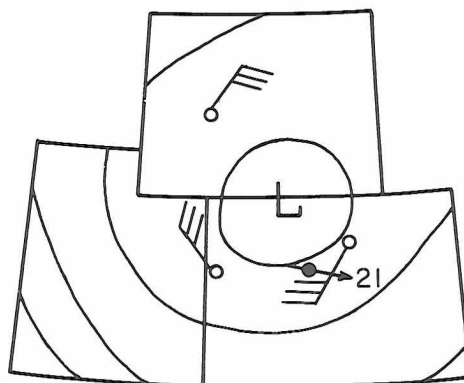
<u>date/time</u>	<u>echo velocity</u>	<u>Climax 500 mb velocity</u>
March		
22/0000Z	WSW/ 44 (mph)	WSW/ 50
22/1200Z	WNW/ 21	W/ 30
23/0000Z	N/ 15	N/ 20
April		
19/0000Z	SSW/ 42	SW/ 40

Precipitation Intensities

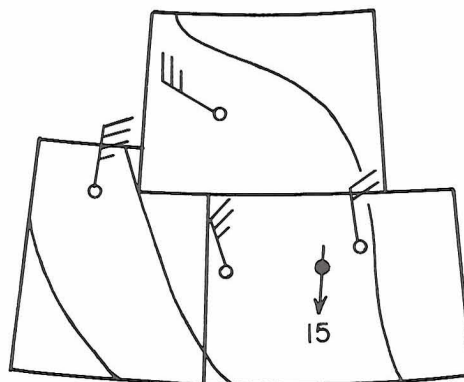
The precipitation intensity was determined by measuring the amount of precipitation which fell in a known period of time. The precipitation was collected on a sheet of plastic of known weight which was placed in an unobstructed area where the snow could deposit on it uniformly. The sheet and its contents were collected



0000 Z
MARCH 22, 1966



1200 Z
MARCH 22, 1966



0000 Z
MARCH 23, 1966

FIGURE 5 500 MB SEQUENCE SHOWING RADAR
ECHO MOVEMENT

and weighed at intervals. By knowing the cross-sectional area of the sheet and the mass of precipitation, the depth of water accumulated per unit time was calculated. The precipitation rate is shown as a function of time in Figure 3.

Error Analysis

In this discussion of data reducing techniques, three sources of major error have been considered. The arguments for eliminating each source are listed below.

1. Often the tops of the clouds are low enough to be obscured on the A-scope by a leakage of the transmitted signal to the receiver. This leakage obscures everything below 3,000 ft above the antenna. For this reason cloud tops below 3,000 ft are reported as "no echo." Since the analysis was concerned with only the stronger echoes and the pulsations of the echoes above the mean height of the echo tops, the absence of the low, weak echoes presented no problem.
2. Through all of the storms observed, the antenna of the search radar was tilted such that there was negligible ground clutter on the PPI. From a topographic map, one may determine the minimum

elevation angle necessary to remove the interference from surrounding mountain peaks. The elevation angle necessary for the beam axis to clear all ground obstacles was found to be 7.5° . To insure that there is no return from a partially filled radar beam, we must consider the beam axis to be elevated above the highest terrain features by one-half the beam width or one-half degree. This gives a total elevation for the beam axis of 8° . At a distance of 10 n mi, the beam axis would be 7,400 ft above Chalk Mountain or 19,400 ft msl.

The mean level of maximum intensity of the clouds was observed approximately 5,000 ft above the radar site. Thus, it was assumed that within 7 n mi of the radar, the amount of echo area lost as a result of the extreme elevation angle was negligible. This reasoning is not valid beyond 7 n mi. However, since 85% of the observed echo area occurred within 4 n mi of the radar (see Table 3), it appears that the amount of echo area undetected between 7 and 10 n mi as a result of the elevation of the radar beam is unimportant compared to the amount undetected as a result of the low reflectivities of the precipitation

(Grant et al., 1965). Hence, it was concluded that the error introduced by the attitude of the radar beam axis was not sufficient to alter the results of this investigation.

3. All of the discussion of radar data is based on the assumption that attenuation of the radar signal passing through precipitation in the form of single crystal snow as compared to agglomerate snowflakes or clusters of snow crystals is of little consequence. In the frequency range for which particles are small in diameter with respect to the wave length, the attenuation is a function of $\sum_{vol} D_i^3$ where D is the water equivalent diameter of the particle (Skolnik, 1962). Therefore, the attenuation decreases as the cube of the particle diameter. This indicates that for small particle snow having water equivalent diameters of 100 to 500 microns, attenuation is much less than in rain where the drop diameters are 10^3 microns and greater. It has also been found that attenuation produced by ice particles in the atmosphere is much less than that caused by rain of equivalent rate of precipitation (Saxton, 1958). This is the result of the difference in the complex

index of refraction of ice as compared to that of water. The ratio of the index of refraction of ice to that of water is $.197/.930$ or approximately $1/5$. These considerations lead to the assumption that attenuation of the radar signal through the snow experienced at higher elevations and colder temperatures is small and may be neglected.

ANALYSIS

Horizontal Echo Distribution

The effect of local terrain on the distribution of $P_j(k)^*$ may be inferred from an investigation of the slopes of the curves in Figure 2. Let us assume that within the clouds the cloud particles are distributed uniformly. The cloud particle size distribution need not be the same for all clouds which means that the maximum reflectivities are not necessarily the same for all clouds. With these assumptions it is implied that a change in the power return, \bar{P}_r , from a cloud will result in a proportional change in the echo area, i.e.,

$$\bar{P}_r = kP_j(k)^* \quad \text{where } k \text{ is a constant.}$$

From radar theory it is known that the power return from a cloud is inversely proportional to the square of the range (Battan, 1959). Combining the two relations, we may express the echo distribution in terms of range,

$$P_j(k)^* = \text{constant}/r^2.$$

This relation has a slope of minus two when plotted on a log-log scale. It can be seen that the slopes of the curves in Figure 2 do not have a slope of minus two for the ranges considered. This implies that the reflectivity gradients are not the same for all clouds. It is also observed that the rate of decrease in $P_j(k)^*$ with range is greater than expected. So, it may be reasoned that

stronger reflectivity gradients occur more frequently than would be expected as the range from the radar site increases. It may be noted that a change of slope toward a more rapid decrease of echo area occurs markedly between 3 to 4 n mi. If the 3 n mi range circle were drawn on a topographic map, it would nearly coincide with two distinct ridges in the terrain; Chicago Ridge to the west and much of the summit of Tenmile Range to the east. The coincidence of the slope discontinuity in Figure 2 and the terrain discontinuities implies that these topographic features probably are effecting the surrounding cloud mass.

The difference in the curves of the different gain steps in Figure 2 is indicative of the distribution of the more intense echoes. As the gain step increases, the receiver gain decreases with a corresponding increase in the minimum detectable signal. Hence, it can be seen that the more intense echo area decreases more rapidly with range than the less intense area observed at full gain.

It is, therefore, concluded that the heaviest precipitation and/or the largest cloud particles are found near the mountain tops.

Vertical Profile

The mean height of the tops of the clouds and the cloud thickness are two of the more interesting features of orographic storms in the Colorado Rockies. Investigators have reported mean tops of

snowstorms associated with frontal systems near Montreal, Canada, to be 13,000 ft msl with a mean thickness of 10,000 ft (Gunn et al., 1954, and Douglas et al., 1957). Measurements of three storms crossing the Rocky Mountains show the mean cloud tops to range between 16,000 ft and 21,000 ft msl. Cloud bases for these storms were visually observed to be between 500 and 1,000 ft. The average observed thickness for these storms, therefore, varied between 4,000 and 9,000 ft. The difference in the mean thickness between the clouds occurring over the mountains and those at lower elevations is the result of vertical shrinking and lateral divergence at the upper levels. This takes place as the storm, crossing the mountains, is lifted nearer the stratosphere, an extremely stable layer of the atmosphere resisting any vertical motion.

Movement

The rate of movement of the radar echoes have been compared to the 500 mb wind velocity over Climax (Table 4 and Figure 5). The results of this comparison indicate that the velocity of the cloud elements investigated is approximately equal to the 500 mb wind velocity. Since the elements investigated were characterized by distinguishable boundaries and small dimensions (radius = 5 n mi), it may be assumed that they were convective cells. It is, therefore, reasonable to conclude that, to a first approximation, the 500 mb

wind acts as a steering wind for the convective elements moving through the orographic cloud mass.

Convective Activity

The detection of organized convective activity is most easily approached by considering the following model. Convective activity is characterized by reflectivities stronger than those of the cloud mass in which it is embedded. This difference in reflectivity is caused by a higher concentration of larger particles. The large particles are the result of the rapid growth of cloud particles due to turbulence and mixing within the cell. This increased reflectivity effectively increases the range of radar detection of the cells.

We are now faced with the task of interpreting the fluctuations of the radar echoes in terms of the passage of convective cells. The vertical-pointing radar will indicate the approach of a convective cell by an increase in the height of the solid and absolute tops. The height of the tops increases until the cell is over the station. As the cell moves from directly over the station, the height of the tops decreases until the height of the top of the parent cloud mass is again reached. This increase in cloud tops is the result of increased radar visibility, which is the result of the increased radar reflectivity of the convective cell. Thus, the passage of a convective cell is seen on the vertical-pointing radar as an increase and subsequent

decrease of the tops of the clouds corresponding to the dimensions and speed of movement of the cell.

Thus far we have discussed the detection of a cell as it passes over the station. The argument for organized activity, i. e., organization in the form of bands, is the regularity of the occurrence of convective cells over the station. Admittedly it is possible but extremely unlikely that convective cells could occur in the orographic cloud with no preferred pattern and pass over the station at regular intervals. However, if the cells were organized into bands spaced at regular intervals, variations of the echo patterns should occur with a period proportional to the distance between the centers of the bands.

Visual inspection of the temporal variations of the cloud patterns, Figure 3, indicates the following. At the beginning of the storm, the major pulsations of the solid tops appear to have a period near 1-1/2 hours. Near the end of the storm the period appears to have increased to 2 hours. Most of these pulsations occur simultaneously with an increase in the maximum horizontal echo range.

The task now becomes one of establishing the quantitative significance of the observed periodicities. A serial correlation was performed on the solid tops and on the maximum horizontal echo range. The time lag used was 15 minutes. A cross

correlation between these two data samples was also performed. In addition the data was spectrally analyzed by the method of Blackman and Tukey (1958). No conclusions could be drawn from the results of any of these calculations. The high persistence and small sample size of the data prohibited meaningful interpretation of the results (Gilman, et al., 1963).

Each data sample was then analyzed to determine the amplitudes of the component harmonic waves. The results of these analyses show a common increase of the amplitude of the wave component having a period of 2-3/4 hours. It is necessary to test this value to determine its statistical significance. This is done by finding the probability that the given ordinate for this period would occur in a sample of random data. The procedure for this test is given in Conrad and Pollack (1962) and will only be outlined here.

A Buys-Ballot schedule was constructed for each data sample for a trial period of 2-3/4 hours. Each row of the schedule was analyzed harmonically for the amplitude of the fundamental wave. The average square amplitude (expectancy) of a single wave was computed from these amplitudes. The amplitude of the period observed on the original periodogram (Figure 6) was then compared to the expectancy. According to Schuster's quantitative test of significance, if the ratio of the original amplitude of the period to the expectancy is 3 or greater then the probability that the

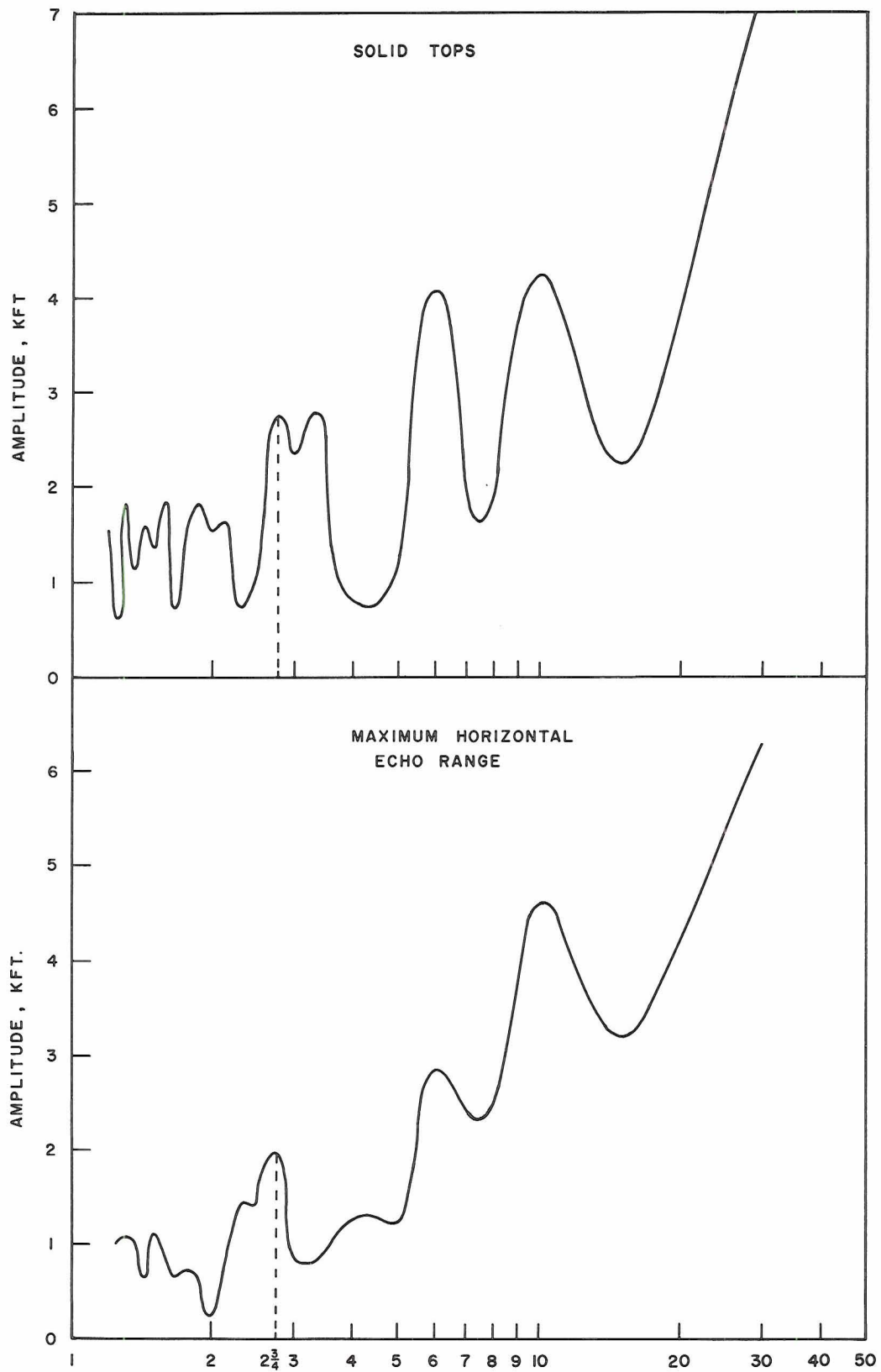


FIGURE 6 AMPLITUDE CONTRIBUTIONS OF HARMONIC WAVE COMPONENTS TO THE TOTAL WAVE FORM

amplitude of the investigated period was produced by chance is less than or equal to 0.01%. For the period of 2-3/4 hours in both data samples the ratio of original amplitude to the expectancy of the single wave was greater than 3. It may be concluded that there is a significant periodicity of the solid tops and the maximum horizontal echo range corresponding to 2-3/4 hours. Therefore, we can reason that the periodicities very probably are the result of the passage of convective bands over the Climax area.

The wind velocity during the storm was constant near 40 mph. This means that the distance between centers of the bands is 110 miles instead of 60 as stated in the model. Though no attempt has been made to explain this discrepancy, there is no reason to argue that the dimensions of the bands should agree exactly with those observed by Elliott and Hovind (1964).

In Figure 3 it can be seen that the history of the precipitation rate corresponds to the fluctuations of the echoes to the extent that the highest precipitation rate occurred simultaneously with the highest solid tops measured during the storm. The precipitation rate is observed to increase to 3.8 and 2.4 mm/hr with the passage of two consecutive bands and drop to less than 1 mm/hr between them. We may conclude from these observations that for this storm the precipitation resulting from the upslope movement of the airmass was small compared to that from the convective bands contained in

the orographic cloud mass. The lack of agreement between the variation of the maximum visible range and the precipitation intensity can be explained by reasoning that the spatial variations of precipitation rate are great within the range of the search radar.

SUMMARY

This investigation has been focused at obtaining information about the structure of winter orographic storms in the Central Colorado Rockies. Observations of three winter storms crossing the Central Rockies reveal definite structural characteristics of the accompanying cloud masses. The storms were monitored on two 3 cm radars located on top of 12,000 ft Chalk Mountain in Central Colorado.

A model of an orographic cloud system assembled from current knowledge, appears to be generally valid for the Central Colorado Rockies. This model incorporates features such as the distribution of precipitation intensity in the vicinity of mountains and the organization and movement of convective activity embedded in the more stable orographically-induced cloud mass. The methods used in this investigation and the results obtained may be summarized as follows:

1. The horizontal distribution of the echoes was determined from the radar film and plotted as a function of range. The results were then compared to the theoretical curve of echo reflectivity versus range obtained from the radar equation. The position of first order discontinuities in the curve of observed data indicate that the heaviest precipi-

tation and most dense clouds occur near the summits of the mountains.

2. The vertical structure of the cloud masses revealed by the vertical-pointing radar shows that the mean tops of the clouds reach from 16,000 to 21,000 ft altitude with an occasional extreme top reaching to 27,000 ft msl. From these observations the mean thicknesses of the clouds were determined to range between 4,000 and 9,000 ft. These values are slightly less than values reported from winter storms over Montreal, Canada, (Gunn et al., 1954, and Douglas et al., 1957). This apparent vertical shrinkage was explained as the result of lifting the storms nearer the stratosphere as they move over the mountains.
3. The movement of well-defined echoes on the PPI was observed and measured. These measurements were then compared to the 500 mb wind velocities and were found to agree. It was concluded that the 500 mb wind was the steering wind for the convective elements embedded in the orographic cloud mass.

4. By comparing the variations of the relative vertical and horizontal radar visibilities, a regular or periodic pattern of alternating increasing and decreasing radar visibility became evident. These simultaneous variations are characteristic of organized convective activity passing over the station. Using harmonic analysis to determine the amplitudes of the harmonic contributions to the total wave pattern, a significant amplitude was found corresponding to a wave with a period of 2-3/4 hours. With an echo speed consistently near 40 mph this period corresponds to a convective band separation of 110 miles.
5. The variations of precipitation intensity that coincided with the passage of the convective bands were very marked. Variations of greater-than-an-order-of magnitude increase in the precipitation intensity were observed as convective bands passed over the station. It was concluded that the amount of precipitation from the embedded convective activity constituted a very large percentage of the total precipitation received from the storm studied.

From this summary one must conclude that the model set forth at the beginning of this paper is an accurate representation of a winter orographic storm cloud system, one exception being that of the distance separating the convective bands is nearly twice that expected.

RECOMMENDATIONS

The physical character of a winter orographic storm is still in the early stages of investigation. Further investigation of the role of the convective activity in the moisture balance of a storm is of primary importance to the field of weather modification. Information necessary to treat this topic is: (1) constant altitude plan position radar information, (2) continuous precipitation intensity records for many locations, and (3) rawinsonde information in the vicinity of the station during a storm.

The convective motions existing in a winter orographic cloud appear to be a major factor in considering the amount of precipitation received from a storm, the particulate distribution in the orographic cloud, and the transport of materials introduced into the base of the cloud. Extensive investigation of this phenomenon is therefore justified and recommended.

BIBLIOGRAPHY

- Atlas, D. and A. C. Chmela, 1957: Physical-synoptic variations of raindrop size parameters. Proc. Sixth Weather Radar Conference, Boston Amer. Meteor. Soc., 21-29.
- Atlas, D. and S. C. Mossop, 1960: Calibration of a weather radar by using a standard target. Bull. Amer. Met. Soc., 41, 377-382.
- Battan, L. J., 1959: Radar Meteorology. Univ. of Chicago Press, Chicago, Illinois, 161 pp.
- Bergeron, T., 1949a: The problem of artificial control of rainfall on the globe, I. Tellus, 1, 1, 32-43.
- Bergeron, T., 1949b: The problem of artificial control of rainfall on the globe, II. Tellus, 1, 3, 15-32.
- Best, A. C., 1950: The size distribution of raindrops. Quart. J. R. Meteor. Soc., 76, 16-36.
- Blackman, R. B. and S. W. Tukey, 1958: The Measurement of Power Spectra. Dover Publications, Inc., New York.
- Blanchard, D. C., 1953: Raindrop size distribution in Hawaiian rains, J. Meteor., 10, 457-473.
- Conrad and Pollack, 1962: Methods in Climatology. Harvard Univ. Press., Cambridge, Massachusetts, 459 pp.
- Douglas, R. H., K. L. S. Gunn and J. S. Marshall, 1957: Pattern in the vertical of snow generation. J. Meteor., 14, 95-114.
- Elliott, R. D. and E. L. Hovind, 1964: On convection bands within Pacific Coast storms and their relation to storm structure. J. Applied Meteor., 3, 143-154.
- Gilman, D. L., F. S. Fuglister and J. M. Mitchell, 1963: On the power spectrum of "red noise." J. Atmos. Sci., 20, 182-184.
- Grant, L. O. and R. S. Schleusener, 1961: Snowfall and snowfall accumulation near Climax, Colorado. Atmospheric Science Technical Paper #17, Colo. State University, Fort Collins.

- Grant, L.O., J. D. Marwitz and C. W. Thompson, 1965: Application of radar to snow surveying. Proc. 33rd Western Snow Conference, Colorado Springs, Colorado, 42-48.
- Gunn, K.L.S., 1955: Snow studies with a zenith-pointing radar. Proc. Fifth Weather Radar Conference, Amer. Meteor. Soc., Boston, 301-305.
- Gunn, K.L.S., 1956: Size distributions of aggregate snowflakes. Sci. Rep. MW-20B, Contract AF19(122)-217, Montreal, McGill University, 9-32.
- Gunn, K.L.S. and T.W.R. East, 1954: The microwave properties of precipitation particles. Quart. J. R. Meteor. Soc., 80, 522-545.
- Gunn, K.L.S. and J. S. Marshall, 1955: The effect of wind shear on falling precipitation. J. Meteor., 12, 339-349.
- Gunn, K.L.S. and J. S. Marshall, 1956: The distribution with size of aggregate snowflakes. J. Meteor., 15, 452-461.
- Gunn, K.L.S., M.P. Langleben and A.S. Dennis, 1954: Radar evidence of a generating level for snow. J. Meteor., 20-26.
- Hindman, E.E., II and R. Rinker, 1966: Continuous snowfall replicator. Submitted to J. Applied Meteor., Aug., 1966.
- Imai, I., 1956: Precipitation streaks and raindrop size distributions. Pap. in Meteor. and Geophys., Meteor. Res. Inst., Japan, 7, 107-123.
- Imai, I., M. Fujiwara and Y. Toyama, 1955: Radar reflectivity of melting snow. Pap. in Meteor. and Geophys., Meteor. Res. Inst., Japan, 6, 130-139.
- Langleben, M.P., 1956: The plan pattern of snow echoes at a generating level. J. Meteor., 13, 544-560.
- Laws, J.O. and D. A. Parsons, 1943: The relation of raindrop size to intensity. Trans. Amer. Geophys. Union, 24, 452-460.
- Ludlam, F.H., 1955: Artificial snowfall from mountain clouds. Tellus, 7, 277-290.

- Marshall, J.S. and W. McK. Palmer, 1948: The distribution of raindrops with size. J. Meteor., 5, 165-166.
- Nakaya, V., 1954: Snow Crystals. Harvard, 508 pp.
- National Academy of Sciences, 1966: Weather and climate modification - problems and prospects, Vol. I, summary and recommendations. Publication No. 1350, National Academy of Sciences, National Research Council, Washington, D. C.
- Rigby, E. C., J. S. Marshall and W. Hitschfeld, 1954: The development of the size distribution of raindrops during their fall. J. Meteor., 11, 362-372.
- Sarton, J. A., 1958: The influence of atmospheric conditions on radar performance. J. Inst. Navigation (London), 11, 209-303.
- Sivaramakrishna, M. V., 1961: Studies of raindrop size characteristics in different types of tropical rain using a simple raindrop recorder. Indian J. Meteor. and Geophys., 12, 189-217.
- Skolnik, Merrill I., 1962: Introduction to Radar Systems. McGraw-Hill Book Co., New York.
- Todd, C. J., 1964: A system for computing ice phase hydrometeor development. Atmospheric Research Group, Altadena, California, ARG 64 Pa-121, 30 pp.
- Wexler, R., 1955: Radar analysis of precipitation streamers observed 25 February, 1954. J. Meteor., 12, 391-393.

APPENDIX

Calibration of SO-12 Radar

Introduction

The objective of radar system calibration is to provide a quantitative means of determining precipitation intensities from radar data. The calibration may be accomplished either by the use of electronic test equipment or by the use of a balloon-borne standard target, (Atlas and Mossop, 1960). The latter eliminates the need of a signal generator for absolute calibration. For the calibration of the SO-12 radar on Chalk Mountain a combination of both procedures have been adopted.

Theory

The calibration is based upon using the echo from a target of known back-scattering cross-section as a standard to which we may compare echoes from precipitation targets. To help understand the calibration procedures it is desirable to recall some pertinent radar theory.

Using the notation of Battan (1959) the equation for the power returned from a single scatterer, such as a balloon-borne target, is:

$$P_r = \frac{P_t G^2 \lambda^2}{(4\pi)^3} \cdot \frac{\sigma}{r^4} = \frac{C \sigma}{r^4} \quad (1)$$

where:

P_r = Power return (watts)

P_t = Transmitted power (watts)

σ = Target back-scattering cross-section (cm^2)

λ = Wave length of the transmitted pulse (cm)

r = Range of target from the antenna (cm)

G = Gain of antenna

and C = "Radar Constant"

When the power is returned from a radar beam filled with hydro-meteors, Equation (1) becomes

$$\overline{P}_r = \frac{C \phi \epsilon h \pi^6 |K|^2}{8\lambda^4} \frac{Z}{r^2} = \frac{C' Z}{r^2} \quad (2)$$

where $k = (m^2 - 1)/(m^2 + 2)$, m being the complex index of refraction.

$Z = \sum \frac{D_i^6}{\text{vol}_i}$, the "reflectivity factor" where D_i is the drop size diameter or the water equivalent diameter in the case of snow particles.

\overline{P}_r = the average power return from a large number of scatterers

where $\pi D/\lambda < 1$. Values of $|K|^2$ for water and ice are known to be

0.93 and 0.197 respectively for wave lengths of 3 to 10 cm and

temperatures of 0C and 20C. For this investigation, atmospheric

attenuation may be considered negligible. This assumption is good

for wave lengths of 3 cm or longer provided that the beam does not

penetrate clouds or precipitation.

From the established calibration curve for the standard target, we would like to be able to determine what reflectivity factor would be necessary for a meteorological target to give the same power return as the standard target at a given range. This is done by equating the known power return of the standard target to the power return from a target of hydrometeors which fill the beam. Solving for the reflectivity factor in terms of range one obtains:

$$Z = \frac{8\lambda^4 \sigma}{\pi^6 \phi \theta h |K|^2 r^2} \quad (3)$$

From Equation (2) it is seen that for a target of multiscatterers the slope of the Z isopleths for \bar{P}_r vs. range is half that of the calibration curve. Hence values of Z as a function of range may be computed from Equation (3) a family of Z isopleths may be drawn through these points on the calibration curve.

It is of interest to determine the gain plus losses of the system. From the calibration curve and Equation (1) the radar constant may be computed, i. e. ,

$$P_r = \frac{C \sigma}{r^4} \quad (4)$$

$$\text{where } C = \frac{P_t G^2 \lambda^2}{(4\pi)^3} \quad (5)$$

Solving for C from (4)

$$C = \frac{P_r r^4}{\sigma} \quad (6)$$

Therefore

$$G = \left[\frac{(4\pi)^3 C}{P_t \lambda^2} \right]^{\frac{1}{2}} \quad (7)$$

The value thus obtained will determine the net gain of the system which is much more useful than the theoretical antenna gain.

Procedure

Before the actual calibration procedure is started amplification linearly of the receiver should be determined. This may be accomplished by finding the variation of the IF bias voltage with the strength of the input signal (dbm). For the radar on Chalk Mountain a TS-147 test set was used to produce the input signal. The strength of this signal could be regulated to any desireable value between -42.0 and -85.0 dbm.

To determine the amplification linearly a graduated series of signals were fed into the receiver and the corresponding IF bias voltage was read on a voltmeter. By allowing for proper coupling and cable losses a curve of IF bias voltage vs. echo intensity (dbm) was obtained. The following is an example of this type of generation:

Magnetron current	6.0 ma
Frequency	9035 mc
Power measurement:	Dial - 14.1 dbm
	Directional coupler 25.3 dbm
	Cable loss 3.2 dbm
	Duty cycle 32.2 dbm
	Peak power 73.2 dbm - 30.0 KW

IF Bias Voltage (volts)	TS-147 Dial Reading (dbm)	Corrected Power* (dbm)
27	-40.0	-68.5
31	-45.0	-73.5
35	-50.0	-78.5
42	-55.0	-83.0
47.5	-60.0	-88.5
52.5	-65.0	-93.5
60	-70.0	-98.5
70	-75.0	-103.5
110	-80.0	-113.5

*Correction - Dial (dbm) \pm directional coupler (dbm) \pm cable loss (dbm)
 = dial (dbm) \pm 28.5.

This calibration is given in Fig. 7 and shows a typical IF bias voltage vs. dbm curve for the SO-12 radar.

Briefly, the calibration procedure is that of observing the echo of a standard target and reducing the receiver gain until the echo is just visible. If the scope brilliance control is held constant, then the threshold gain setting is a reproducible measure of the echo intensity.

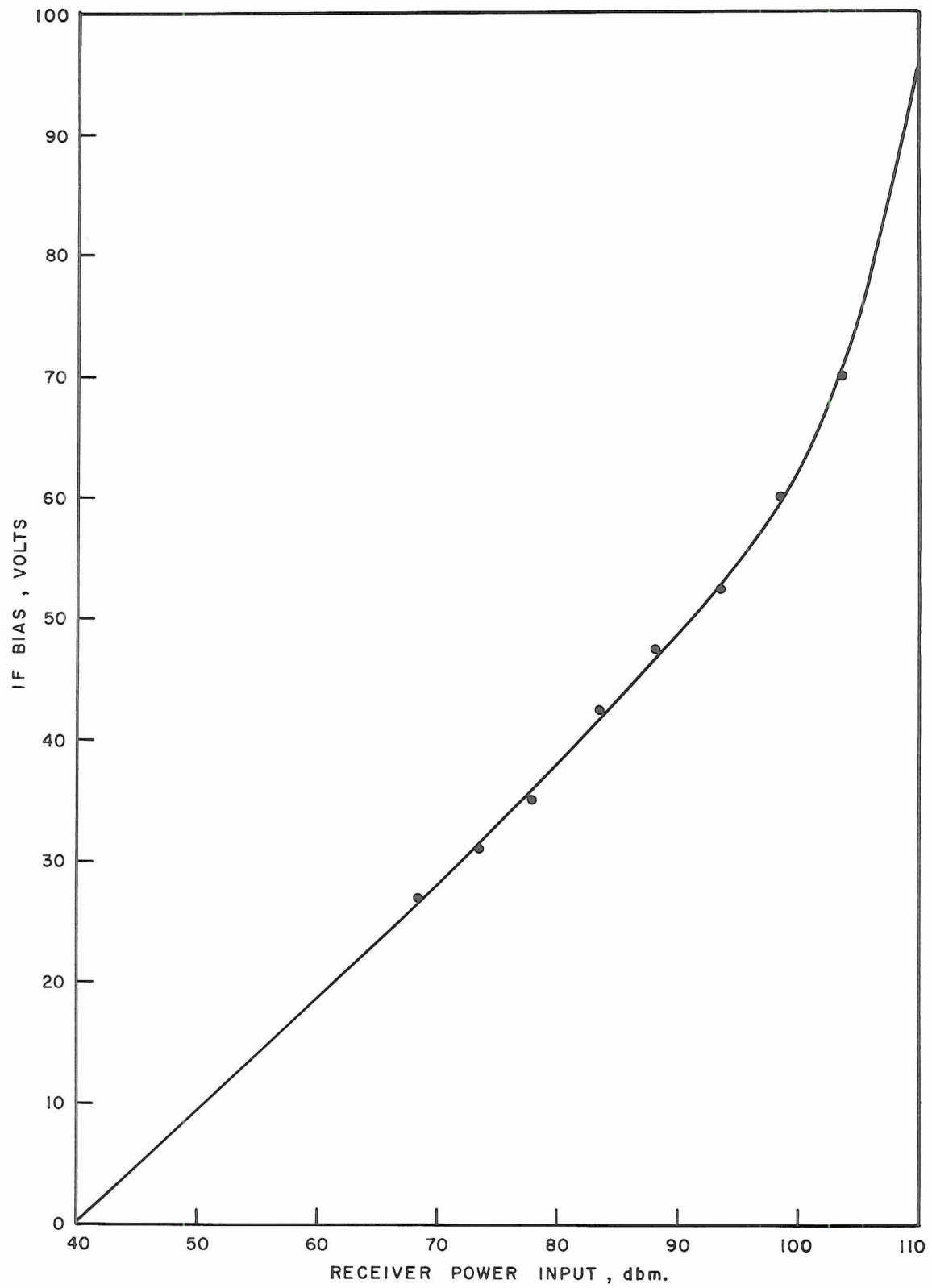


FIGURE 7 RECEIVER LINEARITY CURVE
SO-12 RADAR RECEIVER

In this manner one can compare the threshold gain setting measured for the standard target against similar measurements for a precipitation echo.

The standard target chosen for the calibration of the SO-12 radar was a 12-inch diameter corner reflector made of 1/8-inch thick aluminum. The radar cross section of the corner reflector was found to be $3.02 \times 10^4 \text{ cm}^2$.

On a day conducive to radar visibility, a standard target was suspended from a 950 gram helium-filled balloon which was tethered on a 1,000 foot line. The balloon was tethered various distances from the radar site and the radar was manually sighted on target. Because the normal mode of operation of the radar was the sweep mode with no tracking capabilities, a tethered target was used rather than a target in free flight. The calibration procedure was conducted during the late morning and evening hours when the winds ranged from calm to light and variable, the cloud cover was at a minimum, and the visibility was at a maximum.

When the target was on station, the antenna was manually adjusted until the return signal was strongest. The receiver gain was then reduced to exhibit the threshold signal on the indicator scope and the IF bias voltage was recorded. This reading was taken several times to insure a correct reading. The target was then moved to a different location and the procedure was repeated. Due to the terrain

and characteristics of the radar, only two ranges were used, 1,000 and 2,000 yards. The data points were then plotted on a graph of signal strength vs. range and a curve of best fit was drawn and adjusted such that the slope conformed to the slope of the radar equation (1). This adjustment was very slight.

Using Equation (3) the Z isopleths were then drawn through the calibration curve, (Fig. 8). Since any amplification non-linearly of the receiver has been removed the spacing of the constant Z lines should be equal. It is much more convenient to have a calibration curve which relates range to reflectivity factor for a family of preset gain steps. Figure 9 shows an example of this type of curve which is obtained by changing the axes of Figure 2.

From Equations (4), (5), (6) and (7) the system gain may be calculated as follows:

$$\overline{P}_r = \frac{C \sigma}{r^4} \quad \text{where} \quad C = \frac{P_t G^2 \lambda^2}{(4\pi)^3}$$

For 12" corner reflector $\sigma = 3.0 \times 10^4 \text{ cm}^2$.

Therefore, at $r = 10^4 \text{ yds} = 91.4 \times 10^4 \text{ cm}$

$$\overline{P}_r = -84.2 \text{ dbm} = 3.9 \times 10^{-12} \text{ watts.}$$

Radar Constant:

$$\begin{aligned} C &= \frac{\overline{P}_r r^4}{\sigma} = \frac{3.9 \times 10^{-12} \times (9.1 \times 10^5)^4}{3.0 \times 10^4} \\ &= 9.1 \times 10^7 \frac{\text{w cm}^4}{\text{cm}^2} \end{aligned}$$

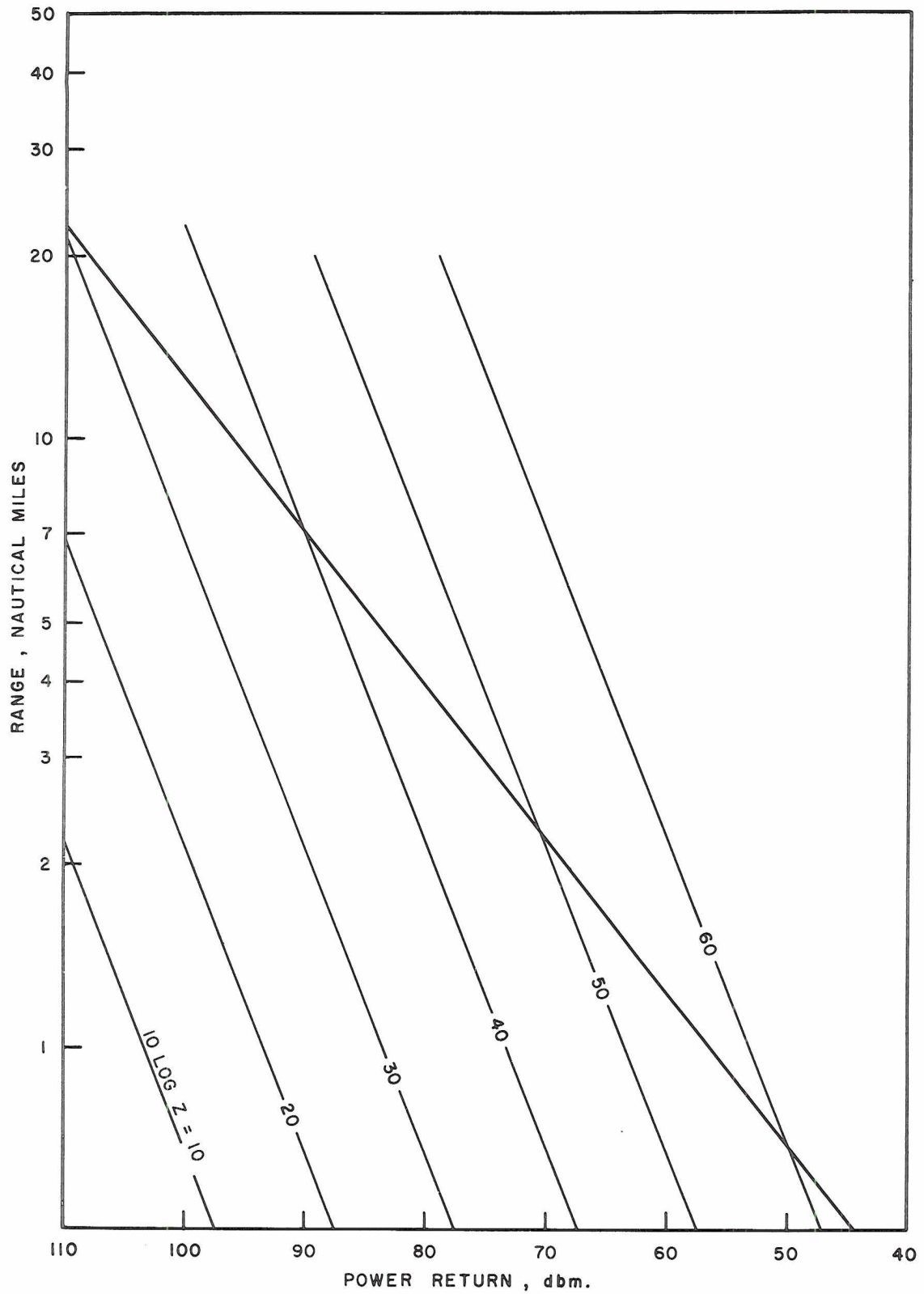


FIGURE 8 SO-12 RADAR CALIBRATION CURVE
USING 12in. CORNER REFLECTOR

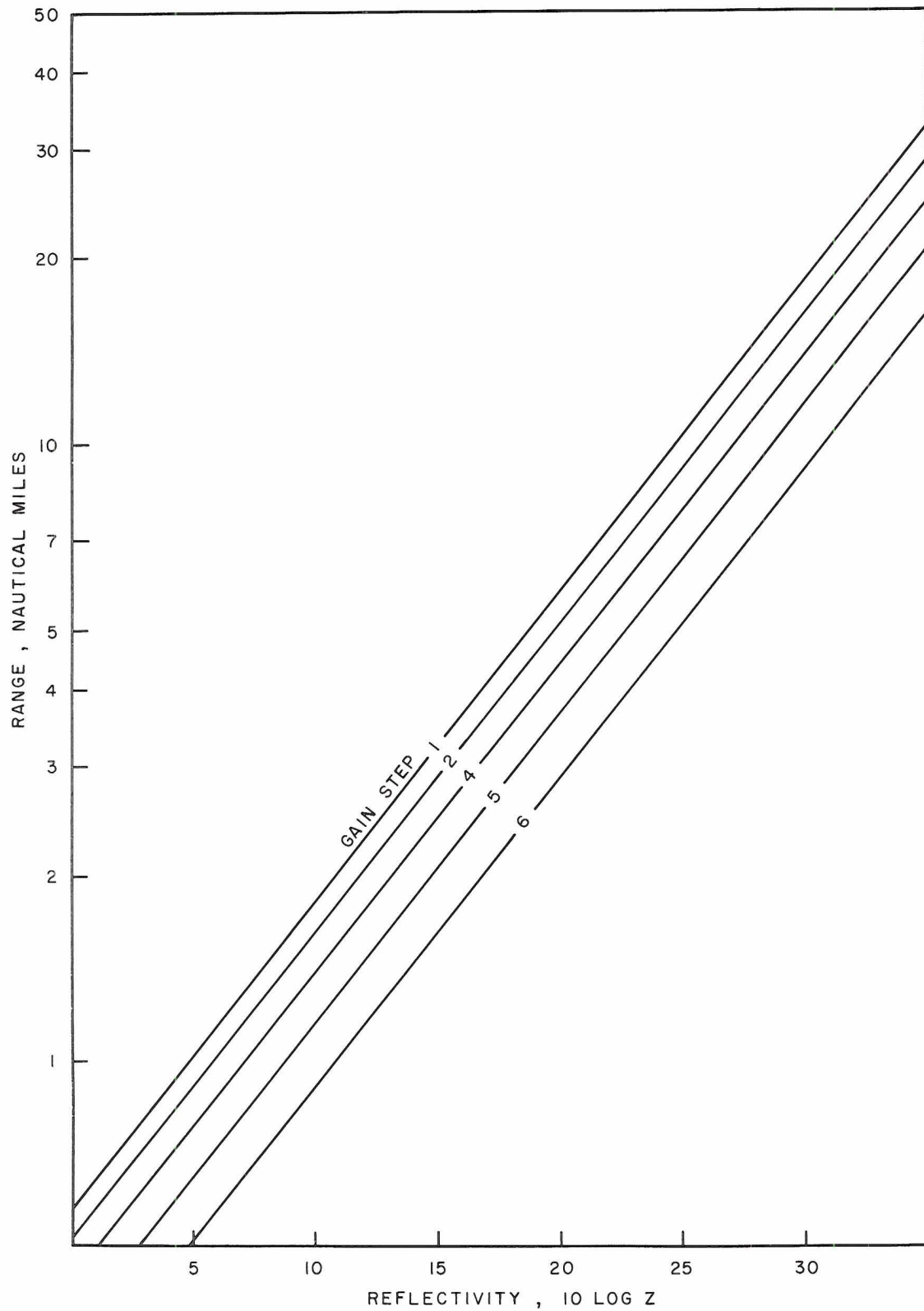


FIGURE 9 CALIBRATION CURVE FOR
MODIFIED SO-12 3cm RADAR

To compute gain (G)

$$P_t = 30 \text{ kw}$$

$$\lambda = 3.31 \text{ cm}$$

$$\text{Therefore, } G^2 = \frac{(4\pi)^3 C}{P_t \lambda^2} = 5.48 \times 10^5$$

$$G = 7.4 \times 10^2 = \underline{28.7 \text{ db.}}$$

Theoretical gain is unknown.

Summary and Recommendations

The appendix has outlined the procedure that to date has been found most satisfactory for the calibration of the SO-12, 3 cm radar located on Chalk Mountain, Climax, Colorado. This procedure allows a more accurate calibration of the equipment than the use of only a signal generator would allow. This is in part the result of not having to assume a rated antenna gain, which, if in error, could cause a serious error in the calculation of Z values.

If the radar equipment is used throughout the year, it is recommended that the equipment be calibrated as outlined above at least once every quarter year of operation. Between these major calibrations the following items should be checked and adjusted at frequent intervals:

- 1) Transmitted power
- 2) Frequency
- 3) Gain step settings
- 4) Min. detectable signal
- 5) Crystal current

Before each major calibration, the following items should be checked:

- 1) Band pass
- 2) Standing wave ratio in the wave guide
- 3) Power losses in the wave guide

Keeping a record of variation of the above mentioned items would significantly increase the reliability of the equipment and the accuracy of any quantitative measurements.